31st Annual International Conference of the IEEE EMBS
Minneapolis, Minnesota, USA, September 2-6, 2009

Neurofeedback of Two Motor Functions Using Supervised Learning-based Real-time Functional Magnetic Resonance Imaging

T. Dorina Papageorgiou, William A. Curtis, Monica McHenry, and
Stephen M. LaConte, *Member, IEEE*

Abstract — **This study examines the effects of neurofeedback provided by support vector machine (SVM) classification-based real-time functional magnetic resonance imaging (rt-fMRI) during two types of motor tasks. This approach also enables the examination of the neural regions associated with predicting mental states in different domains of motor control, which is critical to further our understanding of normal and impaired function. Healthy volunteers (n=13) performed both a simple button tapping task, and a covert rate-of-speech counting task. The average prediction accuracy was approximately 95% for the button tapping task and 86% for the speech task. However, subsequent offline analysis revealed that classification of the initial runs was significantly lower - 75% ($p<0.001$) for button and 72% ($p<0.005$) for speech. To explore this effect, a group analysis was performed using the spatial maps derived from the SVM models, which showed significant differences between the two fMRI runs. One possible explanation for the difference in spatial patterns and the asymmetry in the prediction accuracies is that when subjects are actively engaged in the task (i.e. when they are trying to control a computer interface), they are generating stronger BOLD responses in terms of both intensity and spatial extent.**

I. Introduction

Functional magnetic resonance imaging (fMRI) is a noninvasive technique that measures correlates of neural activity and has been recently evaluated for suitability as a biofeedback signal [1]-[5].

The most common approach to rt-fMRI studies to date has been to track fluctuations in localized regions of interest. Recently, however, we have developed a multivariate, supervised learning approach that can estimate brain states (the sensory/behavioral status of the volunteer) on an image-by-image basis, obtained from the entire brain [6]. This approach has several advantages over localized strategies, including the ability to utilize distributed network patterns that are specific to the behavioral task and individualized to the patient or volunteer.

Motor behavior represents one important target for neurofeedback for applications ranging from skill enhancement to rehabilitation therapy targeted to stroke, traumatic brain injury, neuromuscular diseases, and even speech disorders. An important consideration is that different aspects of motor behavior can involve different networks of the brain. It is therefore critical to study the neural substrates associated with specific motor tasks and to further our understanding of normal and impaired cortical and subcortical motor processes.

In terms of speech therapy, modulating rate of speech is a treatment often used to improve intelligibility. Thus, neurofeedback to enhance control of rate of speech could serve as a potential application in the treatment of dysarthria, which is a neuromuscular speech disorder characterized by poor articulation, and improper speech tempo [7]. To assess the potential for using supervised learning-based rt-fMRI for speech disorders, it is important to characterize the neural correlates of speech tasks and to determine strategies for building accurate predictive models of these tasks.

In the work reported here we examine two different motor tasks, executed with and without neurofeedback: (a) a simple motor task that involves self-paced frequency of right and left index finger tapping on a button box; and (b) a speech production paradigm, which poses considerable demands on motor control networks and assesses rate and effort of automatic, covert speech. Compared with other domains of motor control, such as locomotion or upper limb movements, few data are available on the cerebral organization of motor aspects of speech production that are essential for the fast and accurate execution of orofacial movements synchronized with laryngeal and respiratory functions during speech production [8].

The purpose of this study is to examine classification accuracy and the brain regions that contribute to this accuracy both with and without applying neurofeedback machine learning for the button press task and the speech rate control task.

II. Materials and Methods

A. Subjects

Thirteen healthy, right-handed volunteers (4 males, 9 females, mean age = 30.15) were recruited to participate in the following paradigm: (1) right and left index finger tapping on a button box; and (2) fast and slow rates of

Manuscript received April 27, 2009. This work was supported by The Robert and Janice McNair Foundation.

T. D. Papageorgiou is with the Neuroscience Department, Baylor College of Medicine, Houston, TX 77030 USA (e-mail: dorina@cpu.bcm.edu).

W. Curtis, was with the Dept. of Neuroscience, Baylor College of Medicine, Houston, TX 77030 USA. He is now a medical student at Case Western Reserve, Cleveland, OH 44106 USA (e-mail: wac37@case.edu).

M. McHenry is with the Communication Sciences and Disorders Department, University of Houston, Houston, TX 77004 U.S.A. (e-mail: McMHenry@uh.edu)

S. M. LaConte is with the Neuorscience Department, Baylor College of Medicine, Houston, TX 77030 USA, (phone: 713-798-8499; fax: 713-798-4488; e-mail: slaconte@cpu.bcm.edu).

automatic, covert, sequential counting. Subjects participated in the study after giving their informed consent (Institutional Research Board, Baylor College of Medicine). All subjects were right-handed.

B. fMRI Scanning

Structural and functional brain imaging was performed on a 3.0 T Siemens Allegra (Siemens, Erlangen, Germany). T1-weighted anatomical images were acquired with a transversal orientation with 1 × 1 × 1 mm^3 voxel volume (MPRAGE: 192 axial slices; TR 1200ms; TE 2.93ms; FOV 245mm; Flip Angle 12°). For fMRI, 30 axial slices were acquired for each 8.5 min run with a gradient echo sequence (TR 2000 ms; TE 31 ms; resolution, 3.458 × 3.458 × 5.0 mm^3; FOV 220 mm; flip angle 90°).

C. Presentation of Tasks

Both tasks were based on the presentation of visual stimuli to which subjects gave a response covertly (speech task) or by pressing a button on a button box (button task) (Current Designs™, www.curdes.com). Stimuli were generated on a PC and, using a long focal length projector, back projected to a screen which could be seen via a mirror mounted on the MRI head coil. Visual stimuli were developed with a Python-based software package, Vision Egg (http://www.visionegg.org). For rt-fMRI experiments utilizing feedback, a serial (IEEE RS232) port on the scanner's image reconstruction computer was used to output results to the presentation computer and acted as a control signal to the stimulus program.

The experimental session consisted of two runs of a continuous button press task (left vs. right finger), and two runs of a covert speech task (fast vs. slow covert counting). During the scanning session, the first run for each task was used to train a supervised learning model and the second run used this model to classify each brain volume and convert the result into a control signal to provide visual feedback. Specifically, a linear SVM classification model of right vs. left index finger tapping was generated during the first run, after which the subject repeated the task while real-time feedback was provided every two seconds. Next, the same procedure was used for fast vs. slow covert counting. For the feedback runs, the visual display consisted of a slider bar that was horizontal for the button press task and vertical for the covert counting task. The slider bar showed the current classifier output of left vs. right, or fast vs. slow with a magnitude that was proportional to the distance from the decision boundary. The visual display also included a centrally presented score that served as an indicator of cumulative success during the run. Subjects were asked to visually fixate on the centrally presented score and use their peripheral vision to follow the length and direction of the slider bar. For the first runs of each task (which were used to train the SVM models), the stimulus was similar (to control for low-level visual effects) except that the bar was always at its maximum value for the left or right and for the fast or slow conditions, and the score accumulated at the maximum rate.

D. Support vector machine classification of fMRI data

Support vector machine (SVM) classification was used for real-time feedback [6] and for further offline analysis [9]. Classification algorithms attempt to find a decision rule that uses an input vector, $\vec{u}$, to obtain a scalar-valued output class label, v, with $v \in \{-1,+1\}$. The process of estimating the decision rule is called supervised learning, and uses a training data set $\{\vec{u}_r, v_r\}_{r=1,R}$ with a finite number of examples, R. Once the decision rule is determined, test data, consisting of input vectors can be classified by their output values.

The support vector machine (SVM) is one method for classification used in recent fMRI studies [6][9]-[12]. For two classes, the SVM algorithm attempts to find a linear decision boundary (separating hyperplane) using the decision function $D(\vec{u}_r) = (\vec{w} \cdot \vec{u}_r) + w_0$, where $\vec{w}$ defines the linear decision boundary, and is chosen to maximize the boundaries defined by D = +1 and D = -1 (known as the margin) between the two class distributions. In the soft margin formulation (where training data observations are allowed to fall on the wrong or even the opposite boundary), $\vec{w}$ is found by minimizing the sum $\frac{C}{R}\sum_{r=1}^{R}\xi_r + \frac{1}{2}\|\vec{w}\|^2$, where the ξ_r s, are used to penalize the training errors on the wrong side of the margin, and are termed "slack variables." The free parameter, C, controls the degree to which the training errors, averaged over all R observations penalize the minimization.

Once the SVM model is determined from the training image data, independent test data can be classified using,

$$v = \begin{cases} -1 & D(\vec{u}) < 0 \\ +1 & D(\vec{u}) \geq 0 \end{cases}$$

For fMRI, brain state classification uses the experimental design as the class label (fast and slow are assigned unique classes for the speech task data, and left and right are unique classes in the button press data) and an experiment consists of a series of brain images being collected while class labels are changed. The classifier's input vector consists of an appropriate representation of the spatiotemporal image data. In this situation, we have labeled data.

For block design data, it is possible to represent each image as an input vector $\vec{u}$, as described in [6], where the vector components are the intensity values for each brain voxel at the acquisition time. The experimental condition (behavioral state) associated with each $\vec{u}$ defines the class label, v. Note that the training data and testing data are assumed to be spatially and temporally aligned and have the same dimensionality.

E. Classification accuracy and brain mapping

The rt-fMRI experiments were performed without preprocessing. After the experiment, however the data were preprocessed (alignment, spatial smoothing (4 mm), and transformation to percent change) and re-analyzed. In the

laboratory, the designation of which run is used for training and which is classified can be exchanged (see Fig. 1 A), and we explored both combinations. Recalling that subjects performed the second run for each task with neurofeedback, classification of "feedback" runs was possible using the model generated by the first run. In the same manner, classification of "no-feedback" runs used the second run as the training run to classify the first. Percent classification accuracy was calculated [(number of correctly classified images)/(total number of images) × 100] with AFNI [13] using 3dsvm [9]. In addition, spatial maps derived from the SVM linear weight vector [9] were generated. Note that in this paper "feedback" and "no feedback" refer to what was classified (not the training data), thus a "feedback map" actually was generated from the first run of the task. Maps generated were second level group analyses (t-tests of the individual weight vector maps).

III. RESULTS

The average classification accuracy across subjects of fast versus slow covert counting was higher for the feedback run (86.25%) than for the no-feedback run (71.79%) ($p<0.005$) (Fig. 1 B). This was also true for the index finger tapping task; the average classification accuracy across subjects was higher for the feedback run (95.41%) than for the no-feedback run (75.20%) ($p < 0.001$) (Fig. 1 C). Regions from the SVM maps (Fig. 2) are listed on Table I.

TABLE I
fMRI SPATIAL PATTERNS FOR FINGER TAPPING AND COVERT COUNTING TASKS

Right/Left Finger Tapping	Fast/Slow Covert Counting
Region	Region
Feedback > No-Feedback *p = 0.005*	Feedback > No-Feedback *p = 0.01*
L. culmen * L. postcentral gyrus (g)/S1 L. precentral g/M1 L. inferior parietal g L. medial frontal g L. superior frontal g L. inferior occipital g R. middle frontal g	R. insula* R. supramarginal g* R. superior temporal g* R. superior frontal g* R. parahippocampal g* L. middle frontal g* L. posterior cingulate g* L. medial frontal g* L. anterior cingulate* L. medial frontal g (blue)
Right > Left *p < 0.001*	Fast > Slow *p = 0.001*
R. cerebellar lingual g ▲ L. postcentral g/S1 (BA5) ▲ R. lentiform Bil. postcentral g/S1 (BA3) R. medial frontal g R. thalamus L. inferior parietal g (BA40) L. culmen	Bil. lentiform▲ R. sup. temporal g (BA22) ▲ L. declive ▲ L. dentate ▲ L. postcentral g/S1 (BA4) ▲ L. middle occipital R. sup. parietal g (BA7) R. middle frontal g (BA9)

* denotes patterns of activation during feedback
▲ denotes patterns of activation for right finger tapping of the motor task and fast counting for the speech task

IV. DISCUSSION

Interestingly, these tasks measure different aspects of motor function, but also feedback (training with run 1) /no-feedback (training with run 2) activation seems to be dependent on the type and level of task difficulty. In other words, a task that yields a more robust spatial pattern across subjects, such as the button task seems to require an automatic, bottom-up control of execution (visual areas). The speech task however, reflected greater spatial pattern variability across subjects, which could suggest that a more complex task may require executive processing, such as the prefrontal cortex to a greater magnitude than a task of lesser complexity [16]. The group button task maps revealed right tapping areas of the right cerebellar lingual, left postcentral and inferior parietal gyri. Similarly, left finger tapping showed spatial patterns of left culmen, right thalamus/lentiform, right postcentral, and medial frontal gyri activation. Both left and right finger tapping generated lateralized primary somatosensory (S1) patterns, and ipsilateral cerebellar regions. However, it seems that right finger tapping yielded a more efficient recruitment of cortical processing compared to the spatial patterns for left finger tapping. It is possible that this is due to the fact that the subjects were right-handed, which may result in a more robust activation for right-handed tasks.

For the fast versus slow counting task, slow counting seems to suggest an interaction between bottom-up (middle occipital) and top-down (frontal and parietal) sensory mechanisms. This implies that although sequential counting is an automatic task, the performance of this task that helps distinguish, slow from fast requires fronto-parietal activation, responsible for generating top-down attentional control [17]. Fast counting produced a left cerebellar, right superior temporal gyrus, and bilateral lentiform and postcentral gyrus spatial pattern, which may suggest an automatic/bottom-up sensory control to perform the task.

The present study evaluated the effects of feedback on two domains of motor performance, a simple motor finger tapping task and a covert, automatic speech task in healthy controls. In both of these tasks we get significant differences in the spatial patterns generated (which topographically represent the supervised learning model) and in prediction accuracies. These results seem to be dependent on whether the subjects were simply executing the task or additionally trying to control a slider bar interface. While it is difficult to obtain independent behavioral measures in the inner speech task, it is possible to quantify the button presses in terms of rate and consistency. We have noted in some subjects an increase in button press rate and consistency when subjects were receiving feedback (run 2). One possible explanation, then, for the difference in spatial patterns and the asymmetry in the prediction accuracies is that when subjects are actively engaged in the task (i.e. when they are trying to control a computer interface), they are generating stronger BOLD responses in terms of both intensity and spatial extent. Thus if the model weight vector of one run represents a "super-set" of important spatial locations compared to the other run, we would expect adequate pattern matching and thus good prediction accuracy. On the other hand, if one run's model is

a "sub-set" of the other run's data, then we would expect noisier classification results.

ACKNOWLEDGMENT

We wish to thank Dr. Charles Neblett and Ruth Smith for helpful discussions and Jason P. White for his technical support.

REFERENCES

[1] R. C. deCharms et al., "Learned regulation of spatially localized brain activation using real-time fMRI," *Neuroimage*, vol. 21(1), pp. 436-443, Jan 2004.

[2] R. C. deCharms, et al., "Control over brain activation and pain learned by using real-time functional MRI," *Proc Natl Acad Sci U S A.*, vol. 102(51), pp. 18626-31, Dec 2005.

[3] S. Posse, et al., "Real-time fMRI of temporolimbic regions detects amygdala activation during single-trial self-induced sadness," *Neuroimage*, vol. 18(3), pp. 760-780, Mar 2003.

[4] N. Weiskopf, et al., "Physiological self-regulation of regional brain activity using real-time functional magnetic resonance imaging (fMRI): methodology and exemplary data," *Neuroimage*, vol. 19(3), pp. 577-586, Jul 2003.

[5] S. S. Yoo, and F. A. Jolesz, "Functional MRI for neurofeedback: feasibility study on a hand motor task," *Neuroreport,* vol. 13(11), pp. 1377-1381, Aug 2002.

[6] S. M. LaConte, S. J. Peltier, and X. P. Hu, "Real-time fMRI using brain-state classification," Hum Brain Mapping, vol. 28(10), pp. 1033-1044, Oct 2007.

[7] B. E., Murdoch, E. C. Thompson, and D. G. Theodoros, "Spastic dysarthria," in *Clinical management of sensorimotor speech disorders*, M.R. McNeil, Ed., New York: Thieme, 1997, pp. 287-310.

[8] H. Ackermann, and A. Riecker, "The contribution of the insula to motor aspects of speech production: a review and a hypothesis," *Brain Lang.*, vol. 89(2), pp. 320-328, May 2004.

[9] S. LaConte, S. Strother, V. Cherkassky, J. Anderson, and X. Hu, "Support vector machines for temporal classification of block design fMRI data," *Neuroimage*, vol. 26(2), pp. 317-329, Jun 2005.

[10] D. D. Cox and R. L. Savoy, "Functional magnetic resonance imaging (fMRI) "brain reading": detecting and classifying distributed patterns of fMRI activity in human visual cortex," *Neuroimage*, vol. 19(2 Pt 1), pp. 261-270, Jun 2003.

[11] F. De Martino, et al., "Combining multivariate voxel selection and support vector machines for mapping and classification of fMRI spatial patterns," Neuroimage, vol. 43(1), pp. 44-58, Oct 2008.

[12] Z. Wang, A. R. Childress, J. Wang, and J. A. Detre, "Support vector machine learning-based fMRI data group analysis," *Neuroimage*, vol. 36(4), pp. 1139-1151, Apr 2007.

[13] R. W. Cox, "AFNI: software for analysis and visualization of functional magnetic resonance neuroimages," *Comput Biomed Res.*, vol. 29(3), pp. 162-173, Jun 1996.

[14] Krakauer JW, et al., "Differential cortical and subcortical activations in learning rotations and gains for reaching: a PET study," *J Neurophysiol.*, vol. 91(2), pp. 924-933, Feb 2004.

[15] F. X. Graydon, K. J. Friston, C. G. Thomas, V.B. Brooks, and R. S. Menon, "Learning-related fMRI activation associated with a rotational visuo-motor transformation," *Brain Res Cogn Brain Res.*, vol 22(3), pp. 373-383, Mar 2005.

[16] L. Cauller, "Layer I of primary sensory neocortex: where top-down converges upon bottom-up," *Behav Brain Res.*, vol. 71(1-2), pp. 163-170, Nov 1995.

[17] A. F. Rossi, L. Pessoa, R. Desimone, and L. G. Ungerleider, "The prefrontal cortex and the executive control of attention," Exp Brain Res., vol. 192(3), pp. 489-97, Jan 2009.

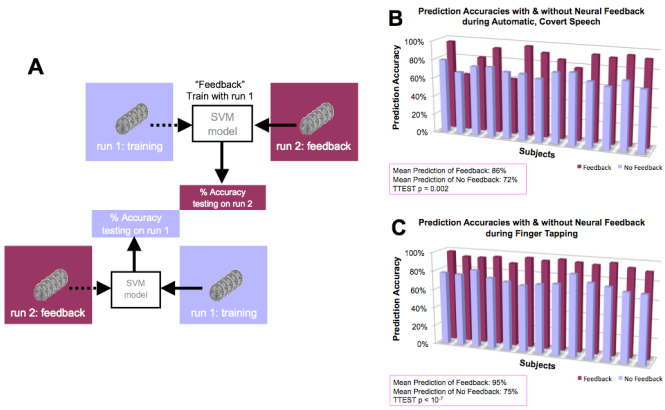

Fig. 1. (A) approach for estimating "feedback" and "no feedback" prediction accuracies. (B) Accuracies for covert speech. (C) Accuracies for button tapping.

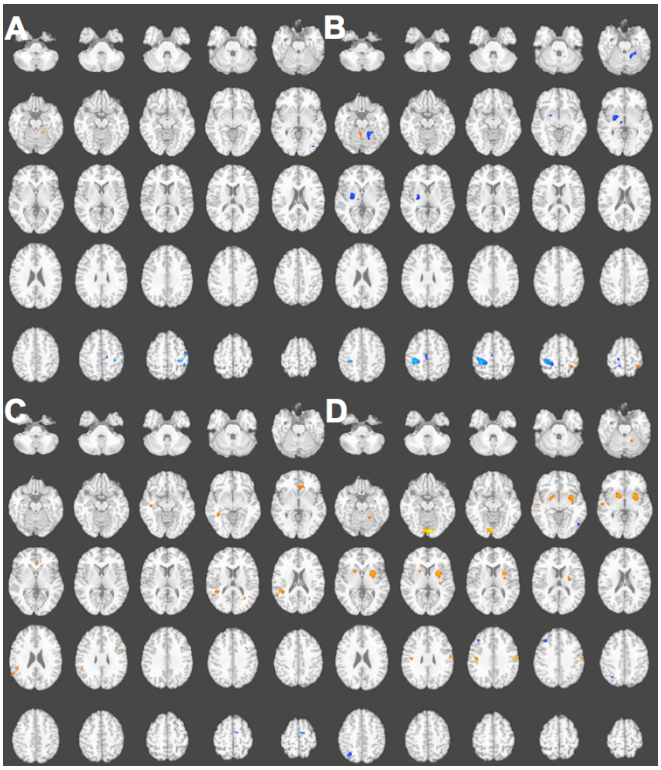

Fig. 2. Group results for SVM models. (A) Feedback vs. no-feedback (training with the first run vs. training with the second run) for the finger tapping task. (B) Right vs. left for the finger tapping task. (C) Feedback vs. no-feedback (training with first run vs. training with the second run) for the covert speech task. (D) Fast vs. slow for the covert speech task.